Contents lists available at ScienceDirect

Transactions of Nonferrous Metals Society of China

36(2026) 386−400

www.tnmsc.cn

Microstructure evolution and mechanical properties of spray-formed 7055 Al alloy subjected to cryogenic rolling

Tian ZHOU [a], Yang-wei WANG [a,b], Jia-wei BAO [a,*], Muhammad Abubaker KHAN [c,**], Ping-luo ZHAO [a], Rui AN [d], Hao ZHANG [e], Mohamed A. AFIFI [f,g]

[a] School of Materials Science and Engineering, Beijing Institute of Technology, Beijing 100081, China;
[b] National Key Laboratory of Science and Technology on Materials under Shock and Impact, Beijing Institute of Technology, Beijing 100081, China;
[c] Beijing Advanced Innovation Center for Materials Genome Engineering, University of Science and Technology Beijing, Beijing 100083, China;
[d] Tangshan Research Institute, Beijing Institute of Technology, Tangshan 063099, China;
[e] Jiangsu Haoran Spray Forming Alloy Co., Ltd., Zhenjiang 212009, China;
[f] School of Engineering and Applied Sciences, Nile University, Giza 12677, Egypt;
[g] Smart Engineering Systems Research Centre (SESC), Nile University, Giza 12677, Egypt

Abstract: Cryogenic rolling impacts on microstructure and mechanical properties of spray-formed 7055 (SF-7055) Al alloy were investigated. Results show that with the increase of the reduction from 20% to 80%, the grain of cryogenic rolled SF-7055 Al alloy is elongated to form a fiber texture. Numerous proliferating dislocations in the microstructure accumulate into dislocation walls and cells, and eventually form subgrains. These subgrain boundaries divide the original grain, thereby reducing the grain size. Under severe deformation conditions, they even enable the formation of nanograins. Meanwhile, the Cu-rich precipitates in the matrix are also broken and refined under the action of large rolling stress. In the process of cryogenic rolling, the tensile strength and hardness of SF-7055 Al alloy gradually increase, while the plasticity decreases. Moreover, the fracture morphology of cryogenic rolled SF-7055 Al alloy gradually transforms to the ductile and quasi-cleavage hybrid fracture characteristics with increased reduction.

Keywords: spray-formed Al alloy; cryogenic rolling; microstructure; mechanical properties; nanograins

1 Introduction

As one of the most advanced aviation Al alloys, 7055 Al alloy has extremely high strength, excellent toughness, and improved stress corrosion resistance, and it has been widely used in civil aircraft such as the B777 and A380 [1−3]. To solve the conventional casting 7055 Al alloy composition segregation and coarse grain problems, the spray forming process is considered an excellent solution to improve the comprehensive mechanical properties of 7055 Al alloy. In the spray forming process, rapid solidification of Al alloy droplets can enhance the solid solubility of alloying elements and inhibit grain coarsening, thus eliminating segregation and refining grains [4−6]. A series of studies [7−9] have shown that the average grain size of spray-formed 7055 (SF-7055) Al alloy is only half of that of traditional casting, effectively preventing Zr element segregation. After hot extrusion and T6 treatment, its microstructure becomes more uniform, and its

Corresponding author: *Jia-wei BAO, Tel: +86-13146900638, E-mail: baojiawei993@163.com;
**Muhammad Abubaker KHAN, Tel: +86-15007557154, E-mail: abubaker@ustb.edu.cn
https://doi.org/10.1016/S1003-6326(25)66971-8
Received 25 May 2024; accepted 29 October 2024

tensile strength can reach approximately 730 MPa.

Although the SF-7055 Al alloy has excellent comprehensive mechanical properties, it still has some significant shortcomings, especially its poor deformation ability due to the high alloy content. Under room temperature deformation conditions, the SF-7055 Al alloy undergoes complex stress states, which can readily result in the emergence of edge cracks and other machining defects. Most Al alloys with high alloy content will have defects such as edge cracking during cold rolling [10−12]. Currently, thermal deformation processes are primarily utilized for the forming of SF-7055 Al alloy [13,14]. Although the thermal deformation process of SF-7055 Al alloy has been relatively mature, there remain several pressing issues that require attention. During the thermal deformation process, the alloy grains tend to coarsen, negatively affecting their mechanical properties. Additionally, the increased metal fluidity at high temperatures frequently results in concentrated deformation and local thinning. Subsequently, residual stress and deformation arising from the cooling process can further exacerbate any differences in dimensions. Furthermore, the oxidation and peeling of the Al alloy surface during thermal deformation will also seriously affect its surface quality [15−17]. These adverse effects on the microstructure and dimensional stability of SF-7055 Al alloy caused by the thermal deformation process seriously restrict its industrial production and practical application. Therefore, it is urgent to explore a new way to solve the deformation problem of SF-7055.

As a new technology, cryogenic deformation process can perfectly solve the deformation problem of high-strength Al alloy. In the liquid nitrogen environment (−196 °C), the plastic deformation of Al alloy is more uniform and stable, and the development of micro-cracks is relatively slow, resulting in the superplastic characteristics of Al alloy [18,19]. Meanwhile, due to the inhibition of dislocation motion and dynamic recovery in the cryogenic environment, the substructural density of the Al alloy after plastic deformation increases sharply, which promotes the increase of strength [20,21]. YANG et al [22] conducted cryogenic rolling and room temperature rolling of 7075 Al alloy followed by aging. At an 80% reduction, cryogenic rolling effectively prevented the formation of numerous edge cracks commonly associated with room temperature rolling. Compared with room temperature rolling, the strength of 7075 Al alloy processed by cryogenic rolling exhibits a slight increase, while the uniform elongation is significantly improved by 72%. XIONG et al [23] investigated the influence of cryogenic rolling and room temperature rolling on the mechanical properties and corrosion properties of 7050 Al alloy. Compared with room temperature rolling, cryogenic rolled 7050 Al alloy produces higher ultrafine grain volume fraction and dislocation density. After aging, the strength of 7050 Al alloy processed through cryogenic rolling is nearly 12% higher than that achieved through room temperature rolling, while also exhibiting superior corrosion resistance. Therefore, the application of cryogenic deformation technology in the industrial production of SF-7055 Al alloy has important practical significance. This work probed into SF-7055 Al alloy by cryogenic rolling under different reductions. Using several measurements and data analysis, the microstructure and mechanical properties of cryogenically-rolled SF-7055 Al alloy under different reductions were systematically investigated. The objective is to produce SF-7055 Al alloy sheets with uniformly refined microstructures, fine grain sizes and superior mechanical properties. It is expected to provide a theoretical basis and technical support for the industrial production of SF-7055 Al alloy.

2 Experimental

2.1 Fabrication process of SF-7055 Al alloy

The SF-7055 Al alloy was prepared using an SFZD−5000 spray deposition equipment. The process schematic diagram is illustrated in Fig. 1. The raw material was heated in a crucible furnace to a temperature range of 700−750 °C until it reached a molten state. This molten material was then allowed to flow into the deposition chamber through the control of a stopper rod and subsequently atomized into small droplets by a high-pressure N_2 air flow of 0.6−1.0 MPa. These droplets were deposited onto a rotating substrate located at a distance of 650 mm from the spray nozzle, forming ingots upon impact. The substrate was rotated at a speed of 45−55 r/min, with a return speed of 2−4 mm/min to ensure an effective deposition. The resultant chemical composition of the SF-7055 Al alloy ingot, in mass fraction (wt.%), is as follows: Zn 7.91, Cu 2.30, Mg

1.92, Zr 0.11, Fe 0.07, Si 0.02, and the remainder being Al.

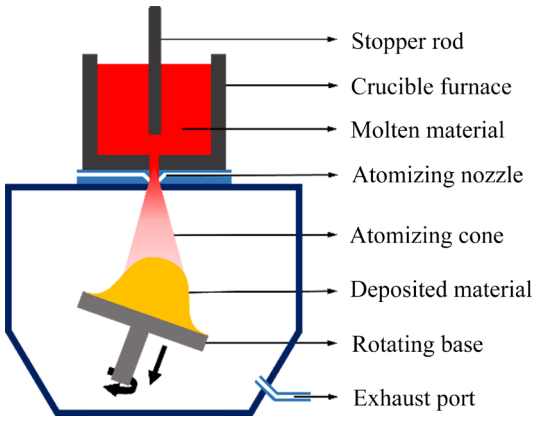

Fig. 1 Schematic diagram of SF-7055 Al alloy preparation

2.2 Cryogenic rolling process, microstructure analysis, and mechanical properties testing methods

The SF-7055 Al alloy ingot was hot-extruded at 430 °C using an 880UST hot extruder. The process was conducted at an extrusion speed of 0.2 mm/s and an extrusion ratio of 15.6 to enhance the material's density. After extrusion, the ingots were cut into plate specimens measuring 100 mm × 100 mm × 5 mm, with care taken to maintain the orientation parallel to the direction of hot extrusion. These plates underwent a solution treatment, initially at 450 °C for 3 h, followed by a temperature increase to 475 °C for a further 3 h, to improve plasticity. Before rolling, the plate specimens were immersed in liquid nitrogen for over 20 min to ensure thorough cryogenic treatment. Rolling was then performed on these specimens parallel to the direction of hot extrusion, with four groups achieving total reductions of 20%, 40%, 60%, and 80%, respectively, using a BFYP−30P rolling mill. During the rolling process each pass reduced the thickness by 5%, followed by a 20-min cryogenic treatment before the subsequent pass.

For microstructural analysis, the cryogenic rolled plates were sectioned into small 10 mm × 10 mm pieces. The samples were first polished and then etched using Keller's reagent (composed of 95 mL water, 2.5 mL nitric acid, 1.5 mL hydrochloric acid, and 1 mL hydrofluoric acid) for 20 s. The etched samples were examined under a Carl Zeiss Axio Vert.A1 optical microscope (OM). Further, the precipitates were analyzed using a Hitachi S−4800 scanning electron microscope (SEM), equipped with an energy dispersive spectrometer (EDS) for compositional analysis. Electron backscattered diffraction (EBSD) was utilized to characterize the grain boundary and substructure distribution. The transmission electron microscope (TEM) samples underwent a precise grinding process, achieving a thickness of 10 μm, before being subjected to additional thinning using the Gatan 691 ion thinning instrument. For a comprehensive microstructural analysis of the cryogenically-rolled SF-7055 Al alloy across varying degrees of reduction, the FEI Talos F200X TEM was employed. The mechanical properties were assessed by measuring the hardness of the rolled samples using an HVS−30 Vickers hardness tester, applying a 49 N load for 15 s. Hardness testing was performed at five different locations on each sample to calculate the average hardness. Tensile properties were evaluated by cutting specimens from the cryogenically-rolled plates along the transverse direction as depicted in Fig. 2. These specimens were tested using an Instron 5985 universal testing machine to ascertain their quasi-static tensile properties. After testing, the fracture surfaces were examined using the same Hitachi S−4800 SEM to observe the fracture morphology.

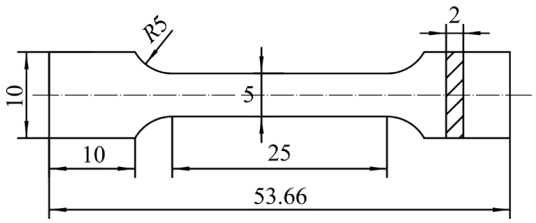

Fig. 2 Schematic diagram of tensile specimen (Unit: mm)

3 Results

3.1 OM images

OM images showing the microstructures of cryogenically-rolled SF-7055 Al alloy at varying degrees of reduction are presented in Fig. 3. At a 20% reduction, the grains of SF-7055 Al alloy exhibit clear signs of plastic deformation, appearing oval as depicted in Fig. 3(a). With an increase in reduction to 40%, the grains elongate, resulting in a higher aspect ratio. Additionally, substructures perpendicular to the rolling direction (RD) begin to emerge within the grains, as illustrated in Figs. 3(b) and (c). Similar substructures were also observed by PANIGRAHI and JAYAGANTHAN [24] in the microstructure of cryogenic rolled 7075 Al alloy. As

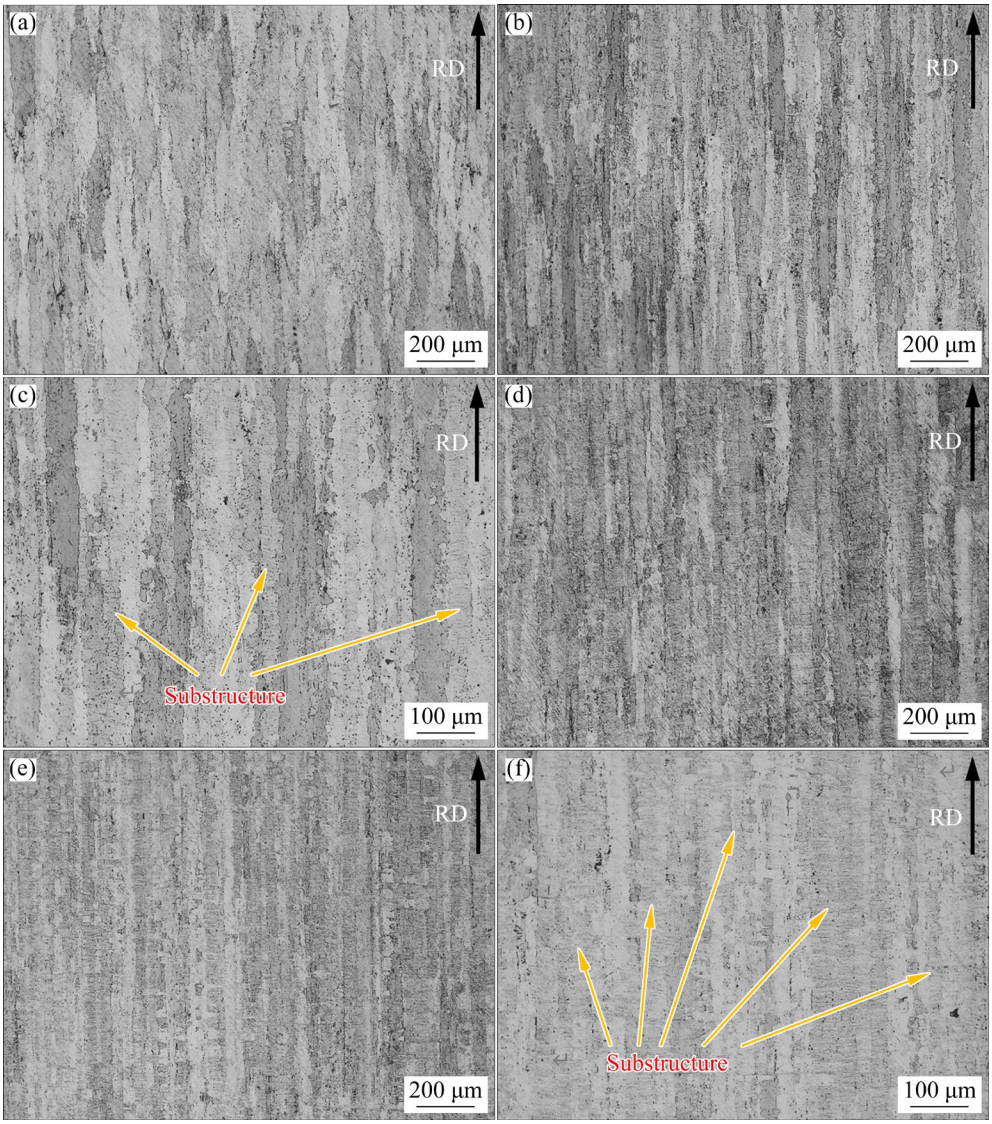

Fig. 3 OM images showing microstructures of cryogenically-rolled SF-7055 Al alloy at reductions of 20% (a), 40% (b, c), 60% (d), and 80% (e, f)

the reduction reaches 60%, the grains transform from oval to a more strip-like shape, and the internal substructure becomes more pronounced, as shown in Fig. 3(d). At the highest reduction of 80%, the strip-like grains break apart, and the grain boundaries become indistinct. Substructures largely dominate the microstructure, visible in Figs. 3(e) and (f). The evolution of microstructures in SF-7055 Al alloy during cryogenic rolling is closely linked to the stress action. At lower reductions, strip grains primarily experience normal stress, which leads to an increase in the aspect ratio. As the reduction level increases, the elongated strip grains become more susceptible to shear stress, leading to an increase in substructures perpendicular to the RD, as reported in Refs. [25,26].

3.2 SEM images and EDS data

SEM images demonstrating the microstructures of cryogenically-rolled SF-7055 Al alloy at different levels of reduction are displayed in Fig. 4. As the reduction increases, the width of the strip grains in the cryogenically-rolled SF-7055 Al alloy gradually narrows. At a high reduction of 80%, the grain boundaries become increasingly indistinct, and a significant number of substructures develop within the grains, as observed in Fig. 4(d). These SEM observations confirm the findings from OM images, providing validation on a finer scale. Additionally, numerous precipitates are observed in the cryogenically-rolled SF-7055 Al alloy. These precipitates, approximately 1 μm in size, are evenly distributed within the grains. As the reduction

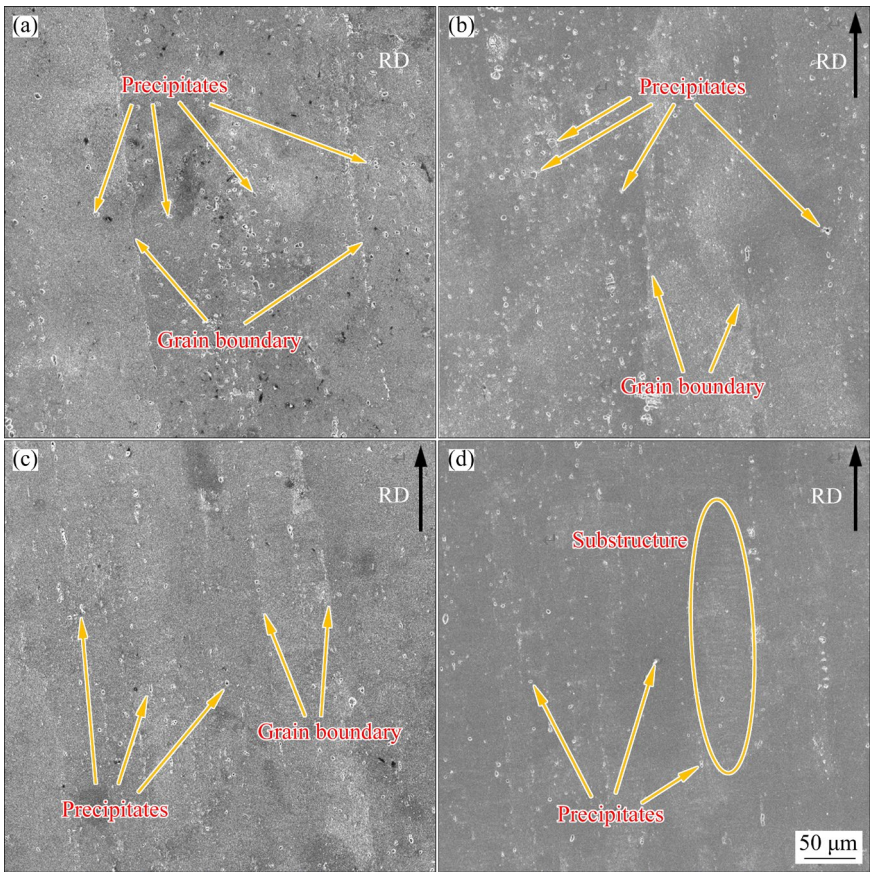

Fig. 4 SEM images showing microstructures of cryogenically-rolled SF-7055 Al alloy at reductions of 20% (a), 40% (b), 60% (c), and 80% (d)

increases, the quantity of these precipitates diminishes, likely due to the substantial plastic deformation causing the precipitates to fracture. EDS analysis further characterizes these precipitates, as shown in Fig. 5. Figure 5(a) shows the SEM image area for the EDS analysis of the Al alloy. Point scanning analysis of a precipitate in Fig. 5(b) confirms that it is rich in Cu element. According to HE et al [27], these Cu-rich precipitates primarily consist of Al_2Cu, AlCu, $AlCu_3$, and Al_4Cu_9. These uniformly distributed Cu-rich precipitates obstruct dislocation movement, thereby enhancing the alloy's strength and hardness. In the Al matrix, the distribution of Mg, Cu, and Zn is relatively uniform, as illustrated in Figs. 5(c−f), which depict element mapping in this region. This uniform distribution of alloying elements in the matrix tends to precipitate into fine nanoparticle precipitates of η and η' phases, further augmenting the strength and hardness of the alloy [28−30].

3.3 EBSD analysis results

EBSD analysis results of the cryogenically-rolled SF-7055 Al alloy under 40% reduction are depicted in Fig. 6. The band contrast map shown in Fig. 6(a) reveals a sharp and clear microstructure morphology, indicating that high-quality diffraction patterns were obtained during rapid data acquisition. In the grain boundary map in Fig. 6(b), black lines delineate high-angle grain boundaries (HAGBs) with misorientation greater than 15°, while red lines indicate low-angle grain boundaries (LAGBs) with misorientation from 2° to 15°. At a 40% reduction, the proportions of HAGBs and LAGBs in the cryogenic rolled SF-7055 Al alloy are 27.5% and 72.5%, respectively. These LAGBs primarily consist of numerous subgrain boundaries formed during the cryogenic rolling process, where dislocations proliferate and align to eventually form dislocation walls, cells and subgrain boundaries. Similar to fine-grain strengthening, the presence of a high density of subgrain boundaries significantly enhances the strength of the SF-7055 Al alloy. The kernel average misorientation (KAM) map in Fig. 6(c) reflects the distribution of local strain and dislocation density under 40% reduction. Here, 92.7% of the local

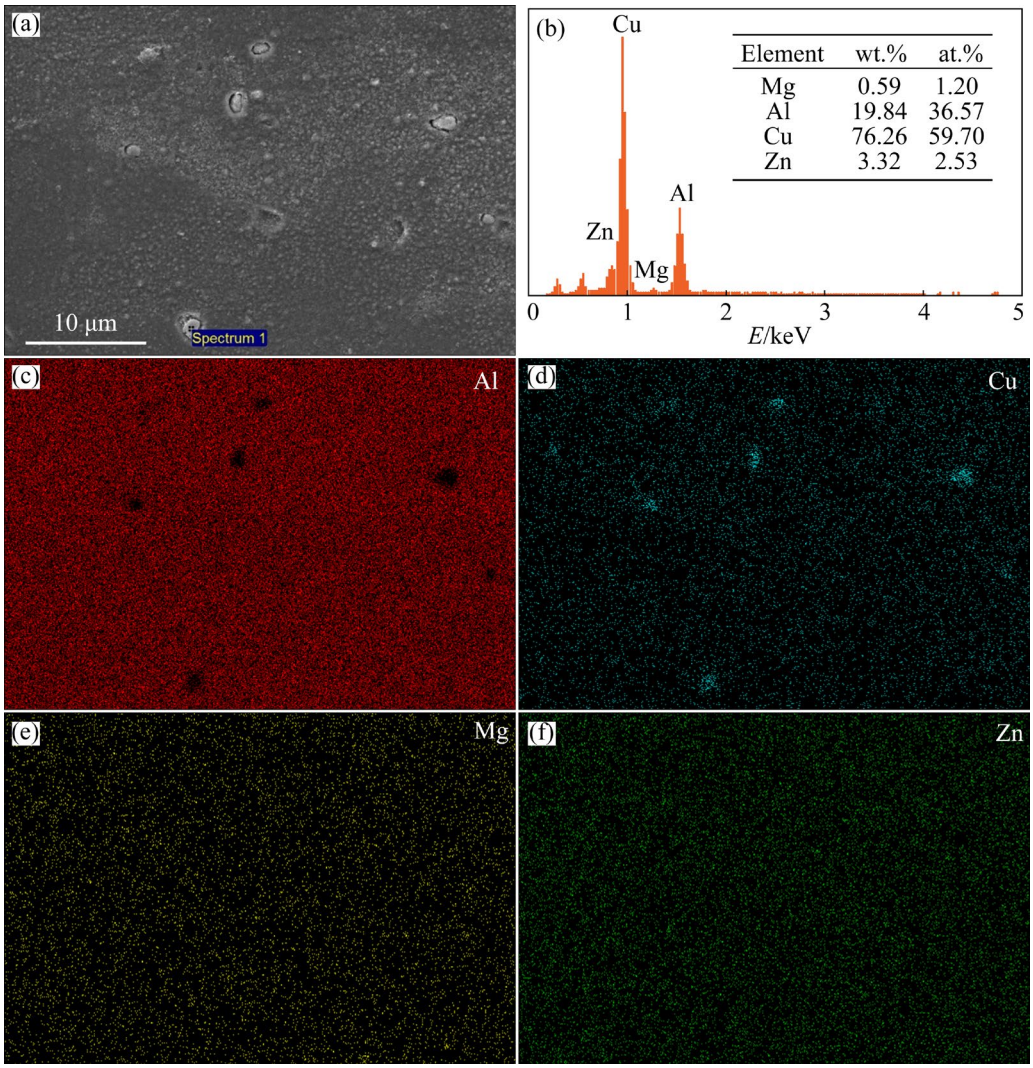

Fig. 5 (a) SEM images of precipitates of cryogenically-rolled SF-7055 Al alloy; (b) EDS element point scanning analysis results of precipitate; (c−f) Element distribution mappings

orientation differences are less than 2°. During cryogenic rolling, the low temperature restricts dislocation movement and entanglement, leading to a uniform dislocation distribution and minimal local strain in the microstructure [31−33]. This uniformity helps to reduce stress concentration during plastic deformation, thereby enhancing plasticity. Figure 6(d) displays the inverse pole figure (IPF) map, which reveals local crystal orientation characteristics under 40% reduction. The texture characteristics of the SF-7055 Al alloy after 40% reduction cryogenic rolling are evident, with the grain orientation showing optimal distribution across all three directions, achieving a maximum texture intensity up to 6.27, as indicated in Fig. 6(e). In the cryogenically-rolled Al alloy, a typical face-centered cubic rolling texture develops, primarily consisting of Copper {112}⟨111⟩, Brass {011}⟨100⟩, and S {123}⟨634⟩ orientations [34,35].

Similarly, EBSD analysis results of the cryogenically-rolled SF-7055 Al alloy under 80% reduction are presented in Fig. 7. In the band contrast map (Fig. 7(a)), black areas signify high dislocation density within these regions, akin to findings reported by KUMAR and KUMAR [36] in cryogenically-rolled 6082 Al alloy with 90% reduction. Compared to the 40% reduction, the density of LAGBs at an 80% reduction significantly increases by nearly 85%, although the density of HAGBs does not show a notable increase but displays disrupted continuity, as illustrated in Fig. 7(b). As the reduction increases, the dislocation density increases, promoting subgrain formation and causing sharp elongation and fragmentation of the original grains into finer grains.

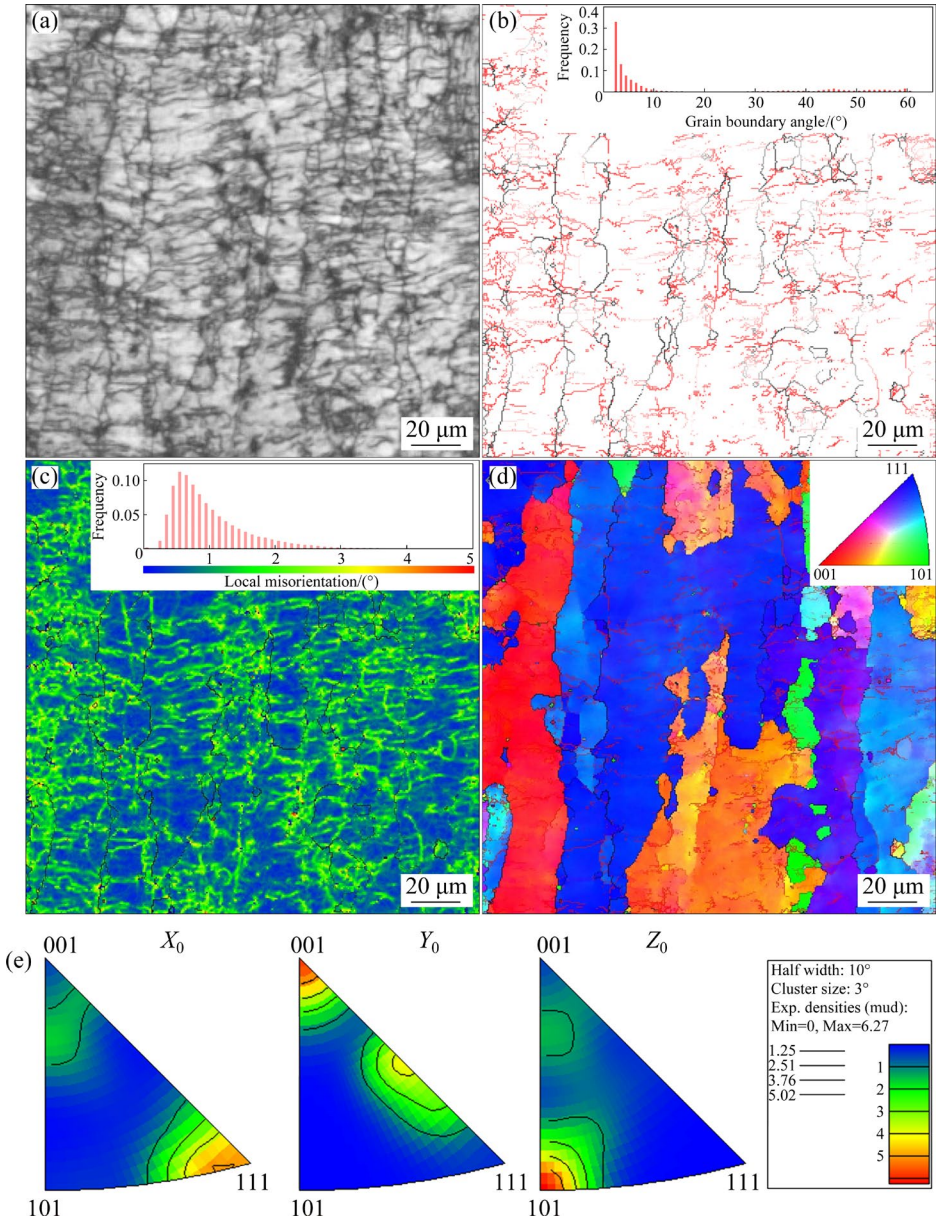

Fig. 6 Band contrast (a), grain boundary (b), KAM (c), grain orientation (d), and IPF (e) maps of cryogenically-rolled SF-7055 Al alloy under 40% reduction by EBSD analysis

The KAM map in Fig. 7(c) indicates that the dislocation density under 80% reduction is higher than that under 40%. The process of cryogenic rolling coordinates plastic deformation through dislocation proliferation and movement. At an 80% reduction, the grain orientation of the cryogenically-rolled SF-7055 Al alloy tends to align consistently towards the ⟨112⟩ direction, correlating with the maximum texture value of 7.45, as shown in Figs. 7(d) and (e).

3.4 TEM images

Figure 8 presents TEM images of cryogenically-rolled SF-7055 Al alloy under different reductions. At a 40% reduction, discontinuous rod-like grain boundary precipitates (GBPs) with a size of approximately 40 nm are observed to be intermittently distributed along the grain boundaries. During the rolling process, solute atoms tend to segregate at the grain boundaries, where they preferentially nucleate to form GBPs, primarily comprising the η phase. Typically, these coarse and discontinuous GBPs contribute to enhancing the corrosion resistance of SF-7055 Al alloy, as reported in Refs. [9,37]. Concurrently, within the grain interiors, uniformly dispersed matrix precipitates (MPts) are visible. These MPts exhibit a short rod-like morphology with

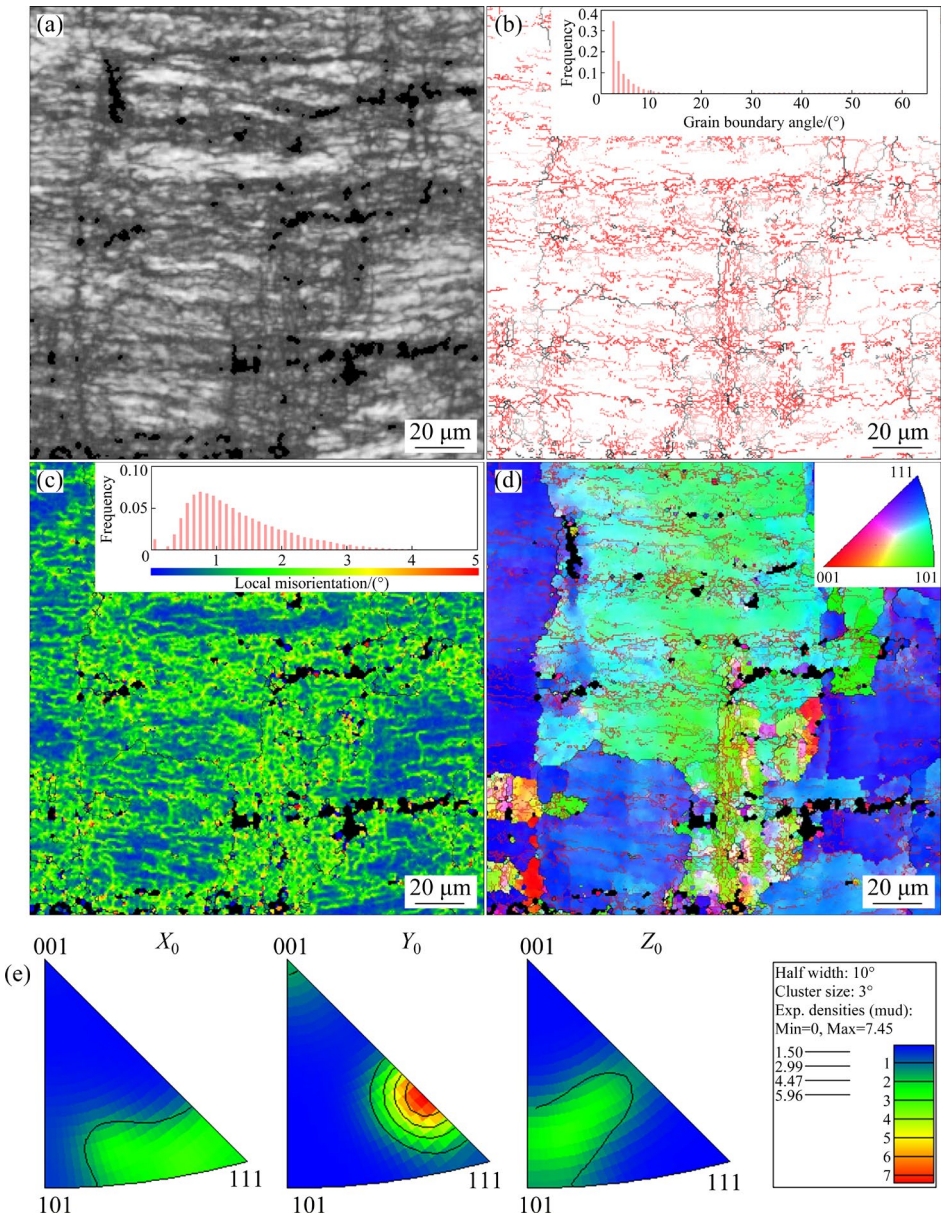

Fig. 7 Band contrast (a), grain boundary (b), KAM (c), grain orientation (d), and IPF (e) maps of cryogenic rolled SF-7055 Al alloy under 80% reduction by EBSD analysis

a length of approximately 20 nm and are primarily composed of η and η' phases. The precipitation sequence during rolling progresses from a saturated solid solution (SSS) through coherent Zn, Mg(Cu)-rich clusters or Guinier-Preston (G.P.) zones, converting to metastable η' phase (semi-coherent $MgZn_2$), and finally stabilizing into η phase (non-coherent $MgZn_2$), as detailed in Refs. [38,39]. The dispersion of fine η' and η phases significantly enhances the strength of the SF-7055 Al alloy. Through plastic deformation, a large number of dislocations are generated in the SF-7055 Al alloy and aggregate to form dislocation walls, which serve as the basis for the formation of subgrains, as shown in Fig. 8(c). Furthermore, to characterize the crystalline structure features, selected area electron diffraction (SAED) pattern is employed, as depicted in Fig. 8(d). Compared to the 40% reduction, the SF-7055 Al alloy exhibits a higher dislocation density at an 80% reduction. These high-density dislocations further evolve into dislocation cells, resulting in the formation of nanograins in certain regions, as illustrated in Fig. 8(e). Under such extensive deformation, distinct grain boundaries have vanished, completely replaced by a multitude of dislocations. Further SAED pattern of the nanograins regions reveals ring-like patterns, confirming the presence of these refined nanocrystals that exhibit different grain

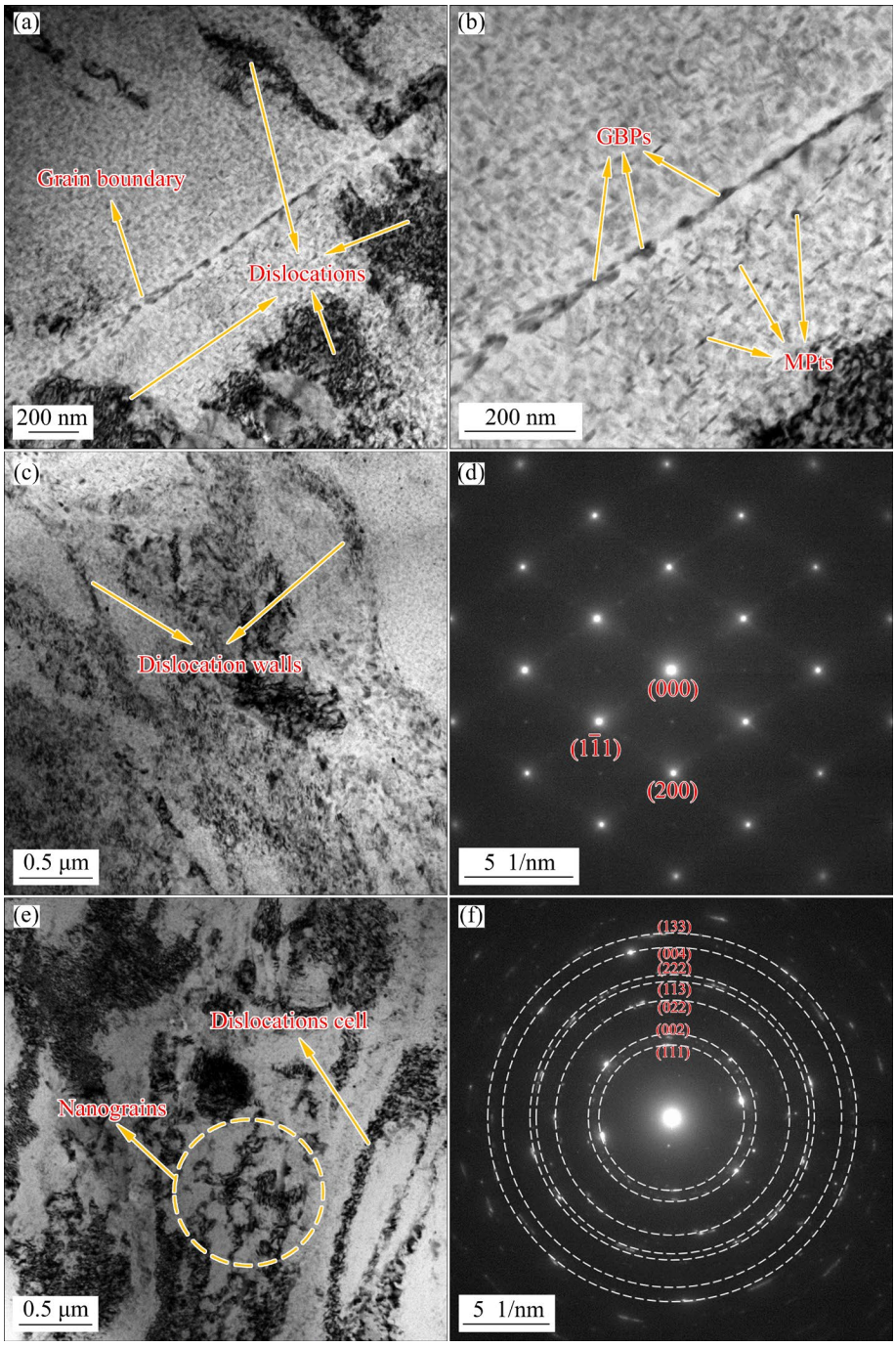

Fig. 8 TEM images of cryogenically-rolled SF-7055 Al alloy, including grain boundaries (a, b), dislocations (c), and SAED pattern (d) under 40% reduction, as well as nanograins (e) and SAED pattern (f) under 80% reduction

orientations, resulting in the broadening of diffraction spots and the formation of continuous diffraction rings (Fig. 8(f)).

3.5 Vickers hardness

Figure 9 illustrates the Vickers hardness of cryogenically-rolled SF-7055 Al alloy under varying degrees of reduction. Initially, the Vickers hardness of the SF-7055 Al alloy in a solid-solution state is HV 147. Upon a 20% reduction, the hardness increases by 24.5% to HV 183. As the reduction continues to increase, there is a corresponding gradual increase in the Vickers hardness values. At an 80% reduction, the hardness further escalates by 44.2% to HV 212. This trend of increasing hardness with greater reduction levels is tightly linked to changes in the microstructure [40−42]. At lower reduction levels, the primary strengthening

mechanism is deformation strengthening. This is driven by an increase in dislocation density and the emergence of deformation textures, which significantly enhance the hardness of the SF-7055 Al alloy, as depicted in Figs. 3(a) and (b). At higher reduction levels, the strengthening mechanism transforms to a synergistic effect of fine-grain strengthening combined with deformation strengthening. The original strip grains break down, leading to the formation of numerous subgrains within the microstructure, contributing to the increased hardness, as shown in Figs. 3(d) and (e). Additionally, the fragmentation of the Cu-rich precipitates during this process also plays a critical role in further enhancing the hardness, as evidenced in Fig. 4.

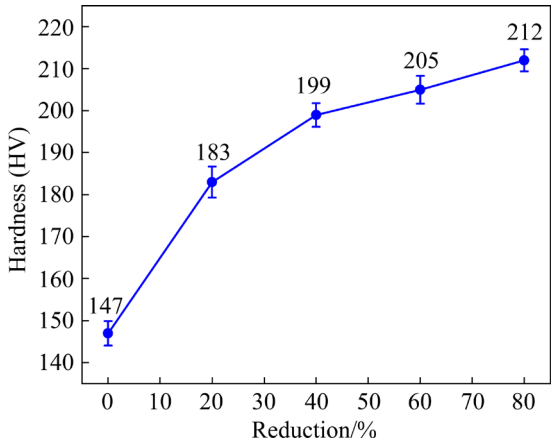

Fig. 9 Vickers hardness of cryogenically-rolled SF-7055 Al alloy under different reductions

3.6 Stress−strain curves

Figure 10 displays the stress−strain curves of cryogenically-rolled SF-7055 Al alloy at various reduction levels. Initially, the SF-7055 Al alloy in solid-solution state shows a tensile strength of 375.6 MPa and an elongation of 21.7%. At a 20% reduction, the tensile strength increases to 625.8 MPa, while the elongation decreases to 16.7%. As the reduction level increases, a consistent pattern emerges: tensile strength continues to rise, and elongation progressively decreases. At an 80% reduction, the tensile strength peaks at 709.1 MPa, an 88.8% increase compared to that of the solid solution state, with elongation maintaining above 10%. The mechanism underlying these changes during cryogenic rolling involves extensive dislocation initiation and evolution, leading to the formation of dislocation walls and cells that further evolve into subgrain boundaries. These microstructural barriers, including dislocation walls, cells, subgrains and grain boundaries, significantly impede dislocation slip caused by plastic deformation, thereby enhancing the material's strength. Moreover, the low temperatures during cryogenic rolling inhibit dislocation movement, resulting in a more uniform distribution of dislocations throughout the microstructure. This high density of uniformly distributed dislocations not only fragments the strip grains but also leads to the formation of numerous subgrains. The high density of these interfaces hinders the propagation of tensile cracks, effectively preserving the material's plasticity. This observation aligns with the findings by MORENO-VALLE et al [43], who noted that reducing the deformation temperature can enhance the plasticity of Al alloys.

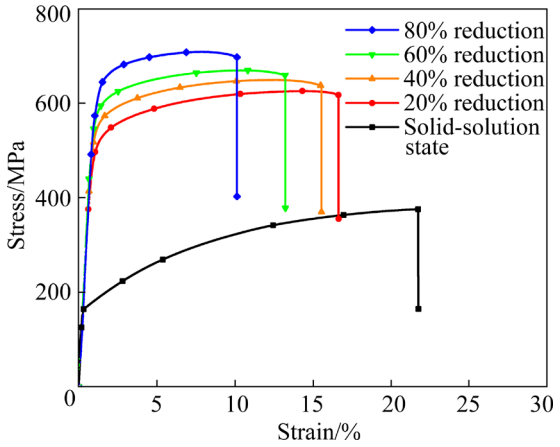

Fig. 10 Stress−strain curves of cryogenically-rolled SF-7055 Al alloy under different reductions

3.7 Tensile fracture morphology

SEM images depicting the tensile fracture of cryogenically-rolled SF-7055 Al alloy under varying degrees of reduction are presented in Fig. 11. At a 20% reduction, the fracture surface of the alloy displays numerous deep dimples, indicative of typical ductile fracture characteristics, as reported in Refs. [44,45]. Concurrently, the presence of elongated grains facilitates the propagation of microcracks along the grain boundaries, resulting in the formation of long tearing edges, as illustrated in Fig. 11(a). As the reduction increases, a deformation texture develops, and the width of the strip grains decreases, leading to shallower dimples and tearing edges in the tensile fracture. In certain regions, a quasi-cleavage plane emerges due to the accumulation of dislocations and the formation of subgrains, as shown

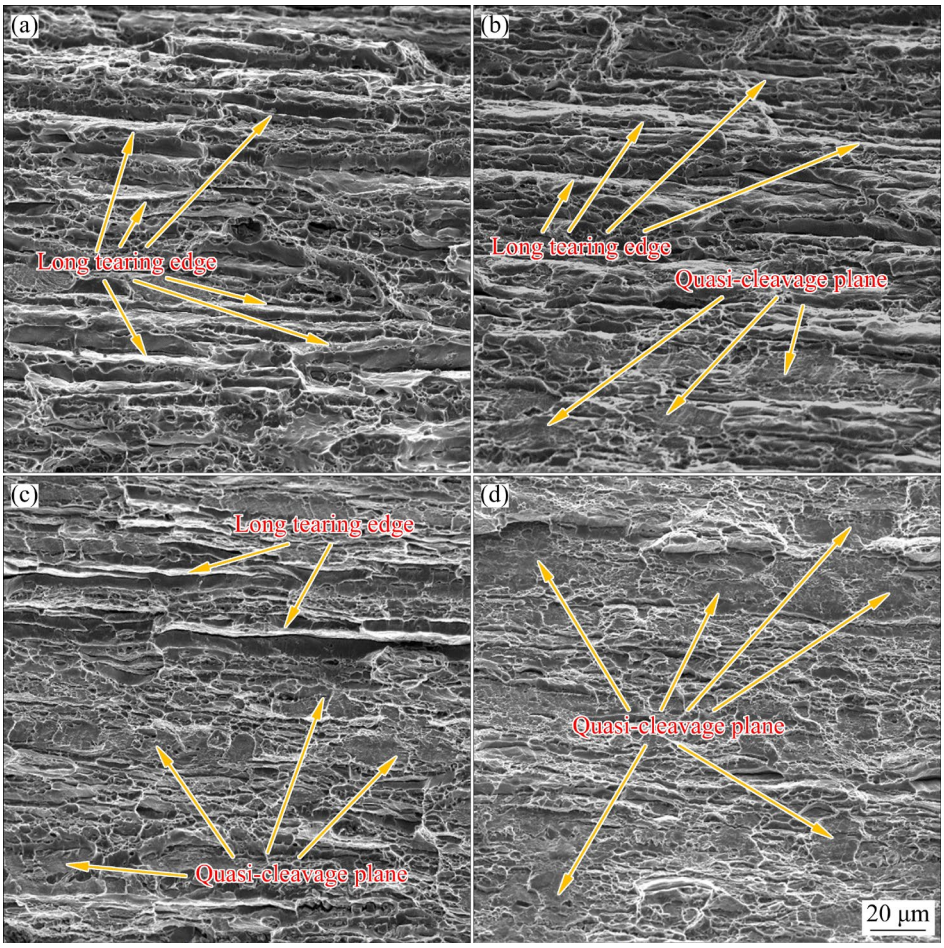

Fig. 11 Tensile fracture morphologies of cryogenically-rolled SF-7055 Al alloy under reductions of 20% (a), 40% (b), 60% (c), and 80% (d)

in Figs. 11(b) and (c). These quasi-cleavage planes evolve from the expansion of cleavage crack nuclei at various sites into cleavage facets, ultimately leading to plastic fracture [46]. At an 80% reduction, the long tearing edge in the tensile fracture vanishes, and a substantial area of a quasi-dissociation surface becomes apparent, as depicted in Fig. 11(d). With further increase in reduction, the dislocation density within the grains of the cryogenically-rolled SF-7055 Al alloy intensifies, resulting in the formation of numerous subgrain boundaries. During the tensile process, a significant number of cleavage crack nuclei appear on these high-energy subgrain boundary surfaces and expand into small cleavage planes. These cleavage planes connect and propagate in conjunction with the primary crack, ultimately leading to fracture. Therefore, as reduction increases, the fracture morphology of the cryogenically-rolled SF-7055 Al alloy gradually shifts towards a combination of ductile and quasi-cleavage fracture characteristics.

4 Discussion

To address the issue of edge cracking in room temperature rolled SF-7055 Al alloy, this study employs a cryogenic rolling process to achieve an SF-7055 Al alloy without apparent defects. Furthermore, the microstructure evolution and mechanical property enhancement of the SF-7055 Al alloy under different rolling reductions are investigated. During the deformation process of cryogenic rolling, the grains of the SF-7055 Al alloy are continuously elongated, as depicted in Fig. 3. At a 40% reduction, once the grains are elongated to a certain extent, they become more susceptible to shear stress than normal stress, resulting in the rearrangement of dislocations perpendicular to the rolling direction [25,26]. This rearrangement gradually leads to the formation of dislocation walls and dislocation cells, ultimately resulting in the emergence of subgrains, as illustrated in Fig. 8(c). As

the reduction further increases to 80%, the original grain boundaries are completely disrupted, and the subgrain boundaries formed by dislocations become the primary constituent of the microstructure. The grain orientations display a tendency to align along the ⟨112⟩ direction, as depicted in Fig. 7(e). At this stage, the grain size of the SF-7055 Al alloy achieves refinement down to the nanometer scale, evidenced by the ring-like diffraction pattern exhibited in Fig. 8(f). The refined nanograins not only enhance the strength but also contribute to a certain extent to the ductility of the SF-7055 Al alloy, thereby mitigating the issue of edge cracking during room temperature deformation.

Along the grain boundaries, rod-like GBPs of approximately 40 nm in size are observed to be intermittently distributed, predominantly composed of η phase, as shown in Fig. 8(a). During the cryogenic rolling process, solute atoms tend to segregate at the grain boundaries, where they preferentially nucleate to form GBPs. In the Al matrix, uniformly dispersed MPts exhibit a short rod-like morphology with a length of approximately 20 nm, consisting mainly of η and η' phases, as depicted in Fig. 8(b). During the rolling process, the precipitation sequence commences from SSS, progressing through coherent Zn, Mg(Cu) clusters or G.P. zones, to a metastable semi-coherent η' phase, ultimately stabilizing into an incoherent η phase [38,39]. The dispersion of fine η and η' phase particles significantly enhances the strength of the SF-7055 Al alloy. In the cryogenically-rolled SF-7055 Al alloy, some Cu-rich precipitates with a size of approximately 1 μm are observed along the grain boundaries, primarily composed of Al_2Cu, AlCu, $AlCu_3$, and Al_4Cu_9, as shown in Fig. 5(b). These Cu-rich precipitates are formed through the continuous migration and accumulation of Cu towards the grain boundary front, resulting from the precipitation of η' and η phases [27]. As the reduction increases, these Cu-rich precipitates undergo fragmentation and refinement due to large plastic deformation, as evidenced in Fig. 4.

Concomitantly, the strength and hardness of cryogenically-rolled SF-7055 Al alloy gradually increase with an increase in the reduction. In the solid-solution state, the SF-7055 Al alloy exhibits a tensile strength of 375.6 MPa, an elongation of 21.7%, and a Vickers hardness of HV 147. After cryogenic rolling with a reduction of 80%, the tensile strength peaks at 709.1 MPa, representing an enhancement of 88.8% compared to that in the solid-solution state, while the elongation remains above 10%, as shown in Fig. 10. The hardness further increases by 44.2% to reach HV 212, as depicted in Fig. 9. These trends in mechanical properties align closely with the observed changes in microstructure. At a lower reduction of 40%, the primary strengthening mechanism is deformation strengthening, driven by the increase in dislocation density and the emergence of deformation textures, as evidenced in Figs. 6(e) and 8(a). However, at a higher reduction of 80%, the strengthening mechanism shifts to a synergistic effect combining fine-grain strengthening and deformation strengthening. This transition is characterized by the fragmentation of the original banded grains, leading to the formation of numerous nanograins within the microstructure, as illustrated in Fig. 8(e). Additionally, the fragmentation of coarse Cu-rich precipitates plays a contributory role in further enhancing the mechanical properties, as shown in Fig. 4. During cryogenic rolling, the low temperature conditions suppress dislocation interaction and annihilation, promoting the formation of subgrains and even nanograins [43]. This improves the stress distribution within the microstructure, enabling SF-7055 Al alloy to achieve a commendable combination of strength and ductility, with minimal compromise in plasticity despite the significant increase in strength. Concurrently, the tensile fracture morphology of SF-7055 Al alloy also undergoes corresponding changes. As the reduction increases, the ductile dimples become shallower, the tearing edge increases and quasi-cleavage planes emerge in certain regions, as depicted in Figs. 11(b) and (c). This transition in fracture morphology indicates a gradual shift from typical ductile fracture to a mixed ductile and quasi-cleavage fracture characteristic.

5 Conclusions

(1) The cryogenic rolling of SF-7055 Al alloy leads to significant microstructural changes, including the elongation of grains, the formation of subgrains, and the development of a deformation texture as the reduction increases. Upon achieving a reduction of 80%, the SF-7055 Al alloy exhibits the formation of nanograins, and the grains transform towards the ⟨112⟩ direction. These transformations

contribute to a continuous increase in hardness, which peaks at an 80% reduction, attaining a Vickers hardness of HV 212, due to the synergistic effects of fine-grain strengthening combined with deformation strengthening.

(2) The tensile strength of the SF-7055 Al alloy significantly increases with higher reductions during cryogenic rolling, while elongation decreases slightly but remains adequate for practical applications. Notably, at a reduction of 80%, the tensile strength attains its peak value of 709.1 MPa, with elongation still maintaining an impressive level above 10%. This improvement in mechanical properties is primarily due to the enhanced dislocation density and the formation of subgrain boundaries, which effectively impede dislocation slip during plastic deformation.

(3) As the degree of reduction in the cryogenic rolling process increases, the fracture morphology of the alloy transforms from predominantly ductile with deep dimples and tearing edges to a hybrid of ductile and quasi-cleavage characteristics. This transition is marked by the emergence of quasi-cleavage planes and the disappearance of long tearing edges at high reduction levels, indicating changes in fracture mechanisms due to evolving microstructure and stress states.

CRediT authorship contribution statement

Tian ZHOU: Methodology, Investigation, Formal analysis, Data curation, Writing − Original draft; **Yang-wei WANG:** Conceptualization, Methodology, Resources, Supervision, Funding acquisition; **Jia-wei BAO:** Conceptualization, Methodology, Investigation, Resources, Funding acquisition; **Muhammad Abubaker KHAN:** Validation, Formal analysis, Data curation, Writing − Review & editing; **Ping-luo ZHAO:** Software, Data curation; **Rui AN:** Software, Data curation; **Hao ZHANG:** Resources, Supervision; **Mohamed A. AFIFI:** Methodology, Supervision.

Declaration of competing interest

The authors declare that they have no known competing financial interests or personal relationships that could have appeared to influence the work reported in this paper.

Acknowledgments

This work was financially and technically supported by the National Key Laboratory Foundation of Science and Technology on Materials under Shock and Impact, Beijing Institute of Technology, China (No. WDZC2024-1).

References

[1] YANG X W, CHENG Q S, DONG Y, YE L Y. Effect of various non-isothermal aging on properties and microstructure of 7055 aluminum alloy [J]. Journal of Materials Research and Technology, 2023, 25: 6275−6287.

[2] ZHANG P, LI Y Y, LIU Y A, ZHANG Y, LIU J X. Analysis of the microhardness, mechanical properties and electrical conductivity of 7055 aluminum alloy [J]. Vacuum, 2020, 171: 109005.

[3] ZUO J R, HOU L G, SHI J T, CUI H, ZHUANG L Z, ZHANG J S. The mechanism of grain refinement and plasticity enhancement by an improved thermomechanical treatment of 7055 Al alloy [J]. Materials Science and Engineering: A, 2017, 702: 42−52.

[4] ZHANG Y C, SUN L B, ZHANG Y Y, XIAO Y, PANG S, YANG L Y. Study on the microstructure and mechanical properties of spray formed and extruded Al−Zn−Mg−Cu alloy [J]. Journal of Materials Engineering and Performance, 2023, 32(3): 955−961.

[5] LI L, ZHOU T T, LI H X, CHEN C Q, XIONG B Q, SHI L K. Effect of additional elements on aging behavior of Al−Zn−Mg−Cu alloys by spray forming [J]. Transactions of Nonferrous Metals Society of China, 2006, 16(3): 532−538.

[6] RAJU K, OJHA S N, HARSHA A P. Spray forming of aluminum alloys and its composites: An overview [J]. Journal of Materials Science, 2008, 43(8): 2509−2521.

[7] ZHAO X J, FAN C Z, YU R H, YUAN P B. Effect of heat treatment on the microstructure and mechanical properties of spray-formed 7055 aluminium alloy [J]. Philosophical Magazine Letters, 2019, 99(3): 102−109.

[8] XIE Z Q, JIA Z H, XIANG K Y, KONG Y P, LI Z G, FAN X, MA W T, ZHANG H, LIN L, MARTHINSEN K, LIU Q. Microstructure evolution and recrystallization resistance of a 7055 alloy fabricated by spray forming technology and by conventional ingot metallurgy [J]. Metallurgical and Materials Transactions A, 2020, 51: 5378−5388.

[9] YANG Y G, ZHAO Y T, KAI X Z, ZHANG Z, ZHANG H, TAO R, CHEN G, YIN H S, WANG M. Effects of hot extrusion and heat treatment on microstructure and properties of industrial large-scale spray-deposited 7055 aluminum alloy [J]. Materials Research Express, 2018, 5(1): 016519.

[10] WANG T, YANG L, HUANG Y F, MA Y Z, WU L, YAN H Y, LIU C, LIU Y, LIU B, LIU W S. Edge crack forming mechanism and the countermeasures in as-sintered 2024 aluminium alloy during cold rolling [J]. Fatigue & Fracture of Engineering Materials & Structures, 2020, 43(12): 2812−2827.

[11] HUO W T, HOU L G, ZHANG Y S, ZHANG J S. Warm formability and post-forming microstructure/property of high-strength AA 7075-T6 Al alloy [J]. Materials Science and Engineering: A, 2016, 675: 44−54.

[12] JEON J G, CHOI K M, LEE S, KANG H, LEE J W, JOO M R, BAE D H. Deformation behavior of a cold-rolled 7075 Al alloy sheet containing small sub-grains with wide low-angle

boundaries [J]. Materials Science and Engineering: A, 2022, 861: 144316.

[13] FENG D, XU R, LI J C, HUANG W J, WANG J T, LIU Y, ZHAO L X, LI C B, ZHANG H. Microstructure evolution behavior of spray-deposited 7055 aluminum alloy during hot deformation [J]. Metals, 2022, 12(11): 1982.

[14] ZHU L Z, LI Z H, ZHANG Z, ZHOU X J. Hot deformation simulation of spray formed 7055 aluminum alloy [J]. Journal of Aeronautical Materials, 2016, 36(1): 18−25.

[15] SHENG X F, YANG Y, YU H C, WU W K, LI K, LIU Y, ZHAO Y F, HE G A. Hot extrusion enhanced homogenization of microstructure in a spray deposition aluminum alloy [J]. Metals, 2020, 10(2): 263.

[16] SCHREIBER J M, OMCIKUS Z R, EDEN T J, SHARMA M M, CHAMPAGNE V, PATANKAR S N. Combined effect of hot extrusion and heat treatment on the mechanical behavior of 7055 AA processed via spray metal forming [J]. Journal of Alloys and Compounds, 2014, 617: 135−139.

[17] JIA Z H, XIE Z Q, XIANG K Y, DING L P, WENG Y Y, LIU Q. Effect of heat treatment and extrusion processing on the microstructure and mechanical properties of spray formed 7055 alloy [J]. Materials Characterization, 2022, 183: 111619.

[18] XIONG H Q, SU L H, KONG C, YU H L. Development of high performance of Al alloys via cryo-forming: A review [J]. Advanced Engineering Materials, 2021, 23(6): 2001533.

[19] CHEN X S, FAN X B, XU A J, YI Z X, YUAN S J. Formability enhancement and deformation mechanism of 2195 Al−Li alloy sheet in cryogenic forming [J]. Materials Characterization, 2023, 196: 112577.

[20] LI C, XIONG H Q, BHATTA L, WANG L, ZHANG Z Y, WANG H, KONG C, YU H L. Microstructure evolution and mechanical properties of Al−3.6Cu−1Li alloy via cryorolling and aging [J]. Transactions of Nonferrous Metals Society of China, 2020, 30(11): 2904−2914.

[21] CHEN X P, MEI L, CHEN D, BAO Z L, LIU Q. The effect of initial aging treatment on the microstructure and mechanical properties of cryorolled 6016 Al alloy [J]. Materials Science and Engineering: A, 2016, 667: 311−316.

[22] YANG S S, LI Z D, ZHOU Y X, TAN Z, KONG C, YU H L. Edge-crack free and high mechanical properties of AA7075 sheets by using cryorolling and subsequent aging [J]. Journal of Alloys and Compounds, 2023, 931: 167556.

[23] XIONG H Q, ZHOU Y X, YANG P, KONG C, YU H L. Effects of cryorolling, room temperature rolling and aging treatment on mechanical and corrosion properties of 7050 aluminum alloy [J]. Materials Science and Engineering: A, 2022, 853: 143764.

[24] PANIGRAHI S K, JAYAGANTHAN R. Development of ultrafine grained high strength age hardenable Al 7075 alloy by cryorolling [J]. Materials & Design, 2011, 32(6): 3150−3160.

[25] DONG H P, GUO F, HUANG W J, YANG X S, ZHU X H, LI H, JIANG L Y. Shear banding behavior of AA2099 Al−Li alloy in asymmetrical rolling and its effect on recrystallization in subsequent annealing [J]. Materials Characterization, 2021, 177: 111155.

[26] MA C Q, HOU L G, ZHANG J S, ZHUANG L Z. Influence of thickness reduction per pass on strain, microstructures and mechanical properties of 7050 Al alloy sheet processed by asymmetric rolling [J]. Materials Science and Engineering: A, 2016, 650: 454−468.

[27] HE W, MA H, SHI Z H, WANG L M, KE D F, TANG C, XIAO W, XUE B Y, WANG J W. Theoretical study on segregation behavior of grain boundaries and precipitated phases in Al−Cu alloys [J]. Materials Science and Technology, 2022, 30(2): 68−74.

[28] REN J, WANG R C, PENG C Q, FENG Y. Multistage aging treatment influenced precipitate characteristics improve mechanical and corrosion properties in powder hot-extruded 7055 Al alloy [J]. Materials Characterization, 2020, 170: 110683.

[29] LIU L L, PAN Q L, WANG X D, XIONG S W. The effects of aging treatments on mechanical property and corrosion behavior of spray formed 7055 aluminium alloy [J]. Journal of Alloys and Compounds, 2018, 735: 261−276.

[30] WANG X D, PAN Q L, LIU L L, XIONG S W, WANG W Y, LAI J P, SUN Y W, HUANG Z Q. Characterization of hot extrusion and heat treatment on mechanical properties in a spray formed ultra-high strength Al−Zn−Mg−Cu alloy [J]. Materials Characterization, 2018, 144: 131−140.

[31] PAN P S, JIANG B, GUO Y, WANG Y, XU H Y, HU M L. Effect of cryorolling on microstructure, conductivities, and mechanical properties of a cast near-eutectic Al−Si−Fe−Mg alloy [J]. Journal of Materials Engineering and Performance, 2024, 33(23): 13112−13119.

[32] KRISHNA N N, TEJAS R, SIVAPRASAD K, VENKATESWARLU K. Study on cryorolled Al−Cu alloy using X-ray diffraction line profile analysis and evaluation of strengthening mechanisms [J]. Materials & Design, 2013, 52: 785−790.

[33] YU H L, LU C, TIEU K, LIU X H, SUN Y, YU Q B, KONG C. Asymmetric cryorolling for fabrication of nanostructural aluminum sheets [J]. Scientific Reports, 2012, 2: 772.

[34] SHI J T, HOU L G, ZUO J R, ZHUANG L Z, ZHANG J S. Cryogenic rolling-enhanced mechanical properties and microstructural evolution of 5052 Al−Mg alloy [J]. Materials Science and Engineering: A, 2017, 701: 274−284.

[35] HUANG Y, PRANGNELL P B. The effect of cryogenic temperature and change in deformation mode on the limiting grain size in a severely deformed dilute aluminium alloy [J]. Acta Materialia, 2008, 56(7): 1619−1632.

[36] KUMAR V, KUMAR D. Investigation of tensile behaviour of cryorolled and room temperature rolled 6082 Al alloy [J]. Materials Science and Engineering: A, 2017, 691: 211−217.

[37] LIU Y, JIANG D M, LI B Q, YANG W S, HU J. Effect of cooling aging on microstructure and mechanical properties of an Al−Zn−Mg−Cu alloy [J]. Materials & Design, 2014, 57: 79−86.

[38] ZHANG P, WANG Y Q, WANG Q. Dynamic evolution of the metastable structure and nano-precipitation of 7055 aluminum alloy under thermal deformation [J]. International Journal of Materials Research, 2018, 109(9): 819−829.

[39] ZUO J R, HOU L G, SHI J T, CUI H, ZHUANG L Z, ZHANG J S. Effect of deformation induced precipitation on grain refinement and improvement of mechanical properties AA 7055 aluminum alloy [J]. Materials Characterization, 2017, 130: 123−134.

[40] VIGNESHWARAN S, SIVAPRASAD K, NARAYANA-

SAMY R, VENKATESWARLU K. Microstructure and mechanical properties of Al−3Mg−0.25Sc alloy sheets produced by cryorolling [J]. Materials Science and Engineering: A, 2019, 740: 49−62.

[41] HOU L G, LIU M L, WANG X D, ZHUANG L Z, ZHANG J S. Cryogenic processing high-strength 7050 aluminum alloy and controlling of the microstructures and mechanical properties [J]. Acta Metallurgica Sinica, 2017, 53(9): 1075−1090.

[42] VIGNESHWARAN S, SIVAPRASAD K, NARAYANA-SAMY R, VENKATESWARLU K. Formability and fracture behaviour of cryorolled Al−3Mg−0.25Sc alloy [J]. Materials Science and Engineering: A, 2018, 721: 14−21.

[43] MORENO-VALLE E C, SABIROV I, PEREZ-PRADO M T, MURASHKIN M Y, BOBRUK E V, VALIEV R Z. Effect of the grain refinement via severe plastic deformation on strength properties and deformation behavior of an A16061 alloy at room and cryogenic temperatures [J]. Materials Letters, 2011, 65(19/20): 2917−2919.

[44] PATHAK M K, JOSHI A, MER K K S, JAYAGANTHAN R. Mechanical properties and microstructural evolution of bulk UFG Al 2014 alloy processed through cryorolling and warm rolling [J]. Acta Metallurgica Sinica (English Letters), 2019, 32(7): 845−856.

[45] BENZERGA A A, BESSON J, PINEAU A. Coalescence-controlled anisotropic ductile fracture [J]. Journal of Engineering Materials and Technology-transactions of the Asme, 1999, 121(2): 221−229.

[46] TAJALLY M, HUDA Z, MASJUKI H H. A comparative analysis of tensile and impact-toughness behavior of cold-worked and annealed 7075 aluminum alloy [J]. International Journal of Impact Engineering, 2010, 37(4): 425−432.

深冷轧制过程中喷射成形 7055 铝合金的显微组织演变和力学性能

周 甜[1]，王扬卫[1,2]，鲍佳伟[1]，Muhammad Abubaker KHAN[3]，
赵平洛[1]，安 瑞[4]，张 豪[5]，Mohamed A. AFIFI[6,7]

1. 北京理工大学 材料学院，北京 100081；
2. 北京理工大学 冲击环境材料技术国家级重点实验室，北京 100081；
3. 北京科技大学 北京材料基因工程高精尖创新中心，北京 100083；
4. 北京理工大学 唐山研究院，唐山 063099；
5. 江苏豪然喷射成形合金有限公司，镇江 212009；
6. School of Engineering and Applied Sciences, Nile University, Giza, 12677, Egypt；
7. Smart Engineering Systems Research Centre (SESC), Nile University, Giza, 12677, Egypt

摘 要：研究了深冷轧制对喷射成形 7055 (SF-7055) 铝合金显微组织和力学性能的影响。结果表明，随着压下量从 20%增加到 80%，深冷轧制 SF-7055 铝合金晶粒被显著拉长，形成纤维组织。显微组织内位错大量增殖塞积形成位错壁和位错胞，并进一步演变成亚晶粒。这些新生的亚晶界将原始晶粒割裂，从而使晶粒尺寸减小。在大变形量条件下，甚至能形成纳米晶粒。同时，在大轧制应力作用下，基体中的富铜析出物也被破碎细化。在深冷轧制过程中，SF-7055 铝合金的抗拉强度和硬度逐渐提高，而塑性逐渐降低。此外，随着压下量的增加，深冷轧制 SF-7055 铝合金的断口形貌逐渐转变为韧性−准解理混合型断裂特征。

关键词：喷射成形铝合金；深冷轧制；显微组织；力学性能；纳米晶粒

(Edited by Wei-ping CHEN)